Retesting of Liquefaction and Nonliquefaction Case Histories from the 1976 Tangshan Earthquake

R. E. S. Moss ; R. E. Kayen ; L.-Y. Tong ; S.-Y. Liu ; G.-J. Cai ; and J. Wu

Abstract: A field investigation was performed to retest liquefaction and nonliquefaction sites from the 1976 Tangshan earthquake in China. These sites were carefully investigated in 1978 and 1979 by using standard penetration test (SPT) and cone penetration test (CPT) equipment; however, the CPT measurements are obsolete because of the now nonstandard cone that was used at the time. In 2007, a modern cone was mobilized to retest 18 selected sites that are particularly important because of the intense ground shaking they sustained despite their high fines content and/or because the site did not liquefy. Of the sites reinvestigated and carefully reprocessed, 13 were considered accurate representative case histories. Two of the sites that were originally investigated for liquefaction have been reinvestigated for cyclic failure of fine-grained soil and removed from consideration for liquefaction triggering. The most important outcome of these field investigations was the collection of more accurate data for three nonliquefaction sites that experienced intense ground shaking. Data for these three case histories is now included in an area of the liquefaction triggering database that was poorly populated and will help constrain the upper bound of future liquefaction triggering curves.

Introduction

The 1976 Tangshan earthquake resulted in widespread liquefaction that was well documented at the time by Chinese researchers (Zhou and Guo 1979; Zhou and Zhang 1979). These reports accurately documented case histories of liquefaction and nonliquefaction by using a standard penetration test (SPT), a cone penetration test (CPT), and borings to acquire subsurface samples for measuring water content, unit weight, and grain size. The CPT measurements however, were made by using what is now an obsolete cone that measured only tip resistance. Current CPT-based liquefaction triggering procedures (e.g., Moss et al. 2006; Youd et al. 2001) require sleeve friction measurements to make accurate liquefaction predictions. This report documents the efforts to reacquire subsurface information with a modern cone capable of measuring tip, sleeve, pore pressure, and shear wave velocity so that these valuable case histories could be included in the worldwide CPT liquefaction database (Moss et al. 2003). The primary focus of these field investigations was on sites providing the most informational content for liquefaction triggering: sites that experienced high estimated ground shaking, and soils that contained high fines content. Highest priority was given to nonliquefaction sites because they tend to be underrepresented in the worldwide liquefaction database.

1976 Tangshan Earthquake

The Tangshan earthquake, $M_S = 7.8$, occurred on July 8, 1976. The epicenter was located in the southern part of the city of Tangshan, and surface fault rupture progressed through the town predominantly to the northeast, with some additional rupture to the southwest. The fault rupture was primarily right lateral strike-slip in nature. The event occurred in the early hours of the morning and the collapse of unreinforced masonry (URM) structures was the primary cause of death that has recently been reassessed to nearly 500,000 lives lost. A detailed compilation of reports on the event and the aftermath can be found in Liu et al. (2002), with additional details on liquefaction in Shengcong and Tatsuoka (1984).

This event occurred in an intraplate region of high seismicity that is dominated by strike-slip faulting. The Global Seismic Hazard Assessment Program's (GSHAP) map of the region (Fig. 1) shows the high seismicity of this region on the basis of historical seismicity and regional tectonics. The source of this crustal stress may be a result of the combined effects of the collision zone to the far southwest between the Eurasian plate and the Indian plate and the subduction zone off the east coast between the Eurasian plate and the Philippine plate. The intraplate region may be an old suture zone among accreted subplate sections (Liu et al. 2002).

The area affected by the earthquake is a piedmont region with many rivers and streams flowing to the Bay of Bo, which is connected to the Yellow Sea. The low hills inland from the current coast are the source of river sediment. It is apparent from the subsurface soil conditions that migrating river channels dominate the depositional environment. Flood plain silts are interlayered with sands having varying silt content. At certain locations, clay deposits exist, indicating either a past lacustrine depositional environment or a sea level rise resulting in a marine depositional environment.

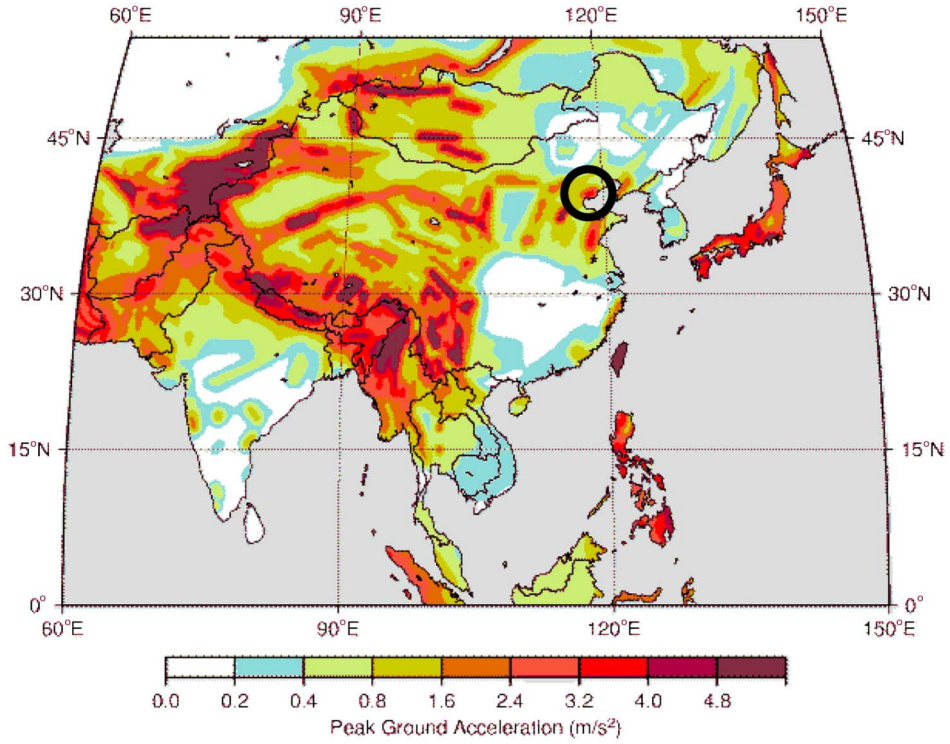

Fig. 1. Seismic hazard map after GSHAP showing a 10% in 50 year estimate of peak ground acceleration; Tangshan region is circled

Most of the liquefaction occurred in the upper few meters of loose- to medium-dense silty fine sand or fine- to medium-clean sand. Most of the nonliquefaction sites were underlain by very dense clean sand. The sites around the city of Tangshan are in the Stone River watershed. The sites in the city of Lutai are in the watershed of the Li Yun River.

Estimates of Strong Ground Shaking

The ground shaking from the event was not well recorded by strong motion instruments. Previous peak ground acceleration (PGA) estimates of Tangshan sites (e.g., Seed et al. 1985; Moss et al. 2006) were based on PGA measurements correlated with reported Chinese intensity measurements. In this study, a calibrated attenuation relationship was used to improve estimates of PGA at each site. The calibration of the attenuation relationship included six instrumental recordings that were not previously available (Liu et al. 2002), and correlated PGA bounds based on Chinese intensity contours. The nearest recording was from a 148 km epicentral distance so the near source fitting was made by using PGA estimates from Chinese isoseismal intensity contours (Fig. 2). Shibata and Teparaska (1988) correlated Chinese intensity to PGA by using the following approximation from the Chinese building code: IX ~ 0.4 g, VIII ~ 0.2 g, and VI ~ 0.1 g. The furthest instrumental recording was from an almost 400 km distance, confirming that an intraplate attenuation relationship best mimics the seismotectonics of the intact basement rock in this region.

To account for the soil nonlinearity from the basement rock to the ground surface, amplification factors for NEHRP Site Class D by Stewart et al. (2003) were applied. Shear wave velocity measurements in this and previous studies indicate that, for the most part, the upper 30 m of soil in this region falls into the Site Class D category. An epicentral distance of 10 km was used as a minimum or saturation epicentral distance because of the uncertainty in the location of the epicenter from the sites. The recordings and

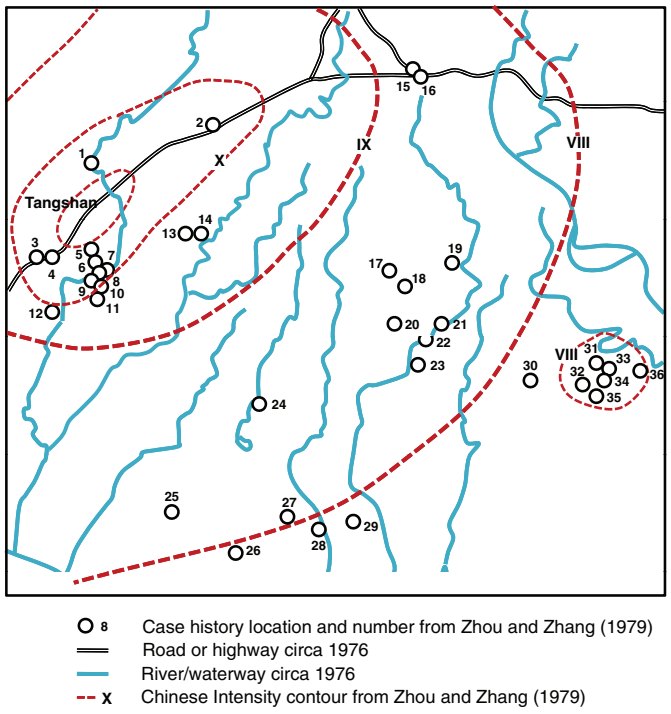

Fig. 2. Chinese intensity map; intensity scale correlated to PGA by using Chinese Building Code; sites with their associated site numbers are shown as circles

the estimated PGA range from Chinese intensity contours were plotted against three well-known intraplate attenuation relationships. The three attenuation relationships evaluated were Atkinson and Boore (1995, 1997); Dahle et al. (1990); and Toro et al. (1997). A depth-to-rupture of 14 km (Liu et al. 2002) was used to convert between hypocentral and epicentral distance. By inspection, the

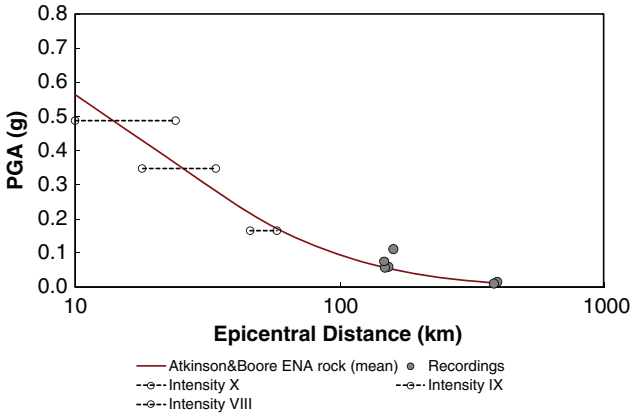

Fig. 3. Atkinson and Boore (1995, 1997) attenuation relationship is shown calibrated to the recordings and estimated rock PGA ranges; attenuation relationship has been converted from hypocentral to epicentral distance by using a depth-to-rupture of 14 km

Atkinson and Boore (1995, 1997) relationship provided the best fit to mean PGA for small and large epicentral distances. This attenuation relationship was then calibrated to the data (Fig. 3) to provide an improved estimate of basement shaking for all sites.

Table 1 shows the sites that were revisited during the 2007 field investigations and the estimated peak ground accelerations derived by using this fitted attenuation relationship method. These estimates are imperfect but are an improvement over the intensity measurements reported in 1978–1979. The uncertainty in this estimation method is accounted for by prescribing a coefficient of variation of 0.4 to the PGA which is consistent with the Moss et al. (2006) data processing techniques for poorly constrained ground motions in which a fitted attenuation relationship is used. This uncertainty translates through the analysis when probabilistic methods are used and will influence the location of the liquefaction triggering curves accordingly.

Table 2 shows revised PGA estimates for the Tangshan sites considered in Moss et al. (2006) that were not reinvestigated during this field investigation. Tables 1 and 2 provide consistent estimates for all the Tangshan sites in the liquefaction database. Sites that were included in Moss et al. (2006) that have been reinvestigated and revised as part of this study are T1, T2, T8, and T10. All other sites (T3, T4, T5, T6, T7, T9, T11, T12, T13, T14, T15, and T16) reinvestigated were not previously considered because no sleeve friction measurements existed and the subsurface soil samples indicated an appreciable fines content.

Data Collection

Data collection was conducted with CPT equipment to measure tip resistance q_c, sleeve friction f_s, pore pressure u, and incremental shear wave velocity V_S. Soil samples were retrieved from certain sites by using a CPT soil sampler and a hand auger to better characterize the soil layers of interest. Spectral analysis of surface wave (SASW) measurements were collected for each site in a separate field investigation (Kayen et al. 2008).

The CPT rig was a Vertek-Hogentogler 200 kN (20 ton) seismic piezocone penetrometer arrangement. The cones (adhering to ASTM 5778) that were used have a 10 cm^2 base area with an apex angle of 60°. A friction sleeve, located behind the conical tip, has a standard area of 150 cm^2. A pressure transducer is located immediately behind the cone tip for measuring pore pressures ($u2$). A temperature sensor is also embedded in the cone, which is primarily used to correct data for thermal offset. A slope sensor is included in the cone design to monitor drift during penetration. A small geophone located inside the cone measures shear wave velocities induced at the ground surface. Data were collected at 50 mm intervals. Seismic shear wave velocity measurements were made every 1 meter during the brief pauses in the cone penetration.

This study has inherent uncertainties because this subsurface investigation occurred so long after the 1976 earthquake. However, reinvestigating liquefaction and nonliquefaction sites of long-past earthquakes has been studied before with success (Moss et al.

Table 1. Estimated Peak Ground Acceleration for Sites Reinvestigated

Sites	Latitude	Longitude	Epicentral distance	Minimum distance	PGA rock	Amplification	PGA soil
T1	N39.68541	E118.20774	8	10	0.56	1.13	0.64
T2	N39.69860	E118.34025	16	16	0.46	1.14	0.53
T3	N39.54396	E118.11207	10	10	0.56	1.13	0.64
T4	N39.54745	E118.13343	9	10	0.56	1.13	0.64
T5	N39.56293	E118.18641	6	10	0.56	1.13	0.64
T6	N39.56293	E118.18641	7	10	0.56	1.13	0.64
T7	N39.55876	E118.19913	6	10	0.56	1.13	0.64
T8	N39.54255	E118.20538	8	10	0.56	1.13	0.64
T9	N39.52287	E118.21356	9	10	0.56	1.13	0.64
T10	N39.53253	E118.20206	9	10	0.56	1.13	0.64
T11	N39.51628	E118.20302	11	11	0.54	1.13	0.61
T12	N39.50315	E118.13576	13	13	0.51	1.14	0.58
T13	N39.58128	E118.32427	13	13	0.51	1.14	0.58
T14	N39.57511	E118.34322	15	15	0.47	1.14	0.54
T15	N39.75145	E118.64855	43	43	0.23	1.20	0.27
T16	N39.75266	E118.68437	46	46	0.22	1.21	0.26
L1	N39.32172	E117.83062	44	44	0.22	1.20	0.27
L2	N39.32503	E117.82849	44	44	0.22	1.20	0.27

Note: All distances are reported in kilometers and PGA in units of gravity.

Table 2. Revised PGA Estimates for Sites Not Reinvestigated during This Field Investigation

Site	Previous PGA estimate[a]	Epicentral distance	PGA rock	Amplification	Current PGA estimate[b]
F13	0.09	101	0.10	1.28	0.12
T19	0.20	49	0.20	1.21	0.25
T21	0.20	49	0.20	1.21	0.25
T22	0.20	47	0.21	1.21	0.25
T30	0.10	63	0.16	1.23	0.20
T32	0.15	70	0.14	1.24	0.18
T36	0.15	77	0.13	1.25	0.16
Y21	0.08	101	0.10	1.28	0.12
Y24	0.09	101	0.10	1.28	0.12
Y28	0.09	101	0.10	1.28	0.12
Y29	0.08	101	0.10	1.28	0.12

Note: This provides consistent median PGA values for all Tangshan sites considered in Moss et al. (2006).
[a]Previous PGA estimate from Moss et al. (2006).
[b]Current PGA estimate derived by using the methods described in this study.

2005). Of primary importance in reinvestigating a previously documented site is the accurate location of the previous subsurface investigations. This is a function of how well the site was documented at the time with maps, coordinates, ground and aerial photos, field notes, references to landmarks, and in this case, the long-term memory of nearby residents. The sites must also be relatively unmodified since the previous investigation.

At the sites in this study, which are generally located in rural agricultural areas, little land development occurred. Locating the sites previously investigated involved driving to the town or landmark named in the logs by Zhou and Gou (1979) and Zhou and Zhang (1979), asking the residents who lived through the earthquake to recall the event and subsequent subsurface investigations, and then, by consensus, determining the location of the previous investigations. This appears to be an ad hoc method, but keep in mind the impression that a devastating earthquake and aftermath can have on people. Not only was this probably the largest natural disaster these people experienced, but in the aftermath, they were host to a group of investigators with government credentials and large testing equipment who asked them detailed questions about their experiences and then drilled into the ground to collect subsurface information. At most sites, little disagreement among the rural residents as to the whereabouts of the previous testing location arose, and when there was disagreement, the difference was usually

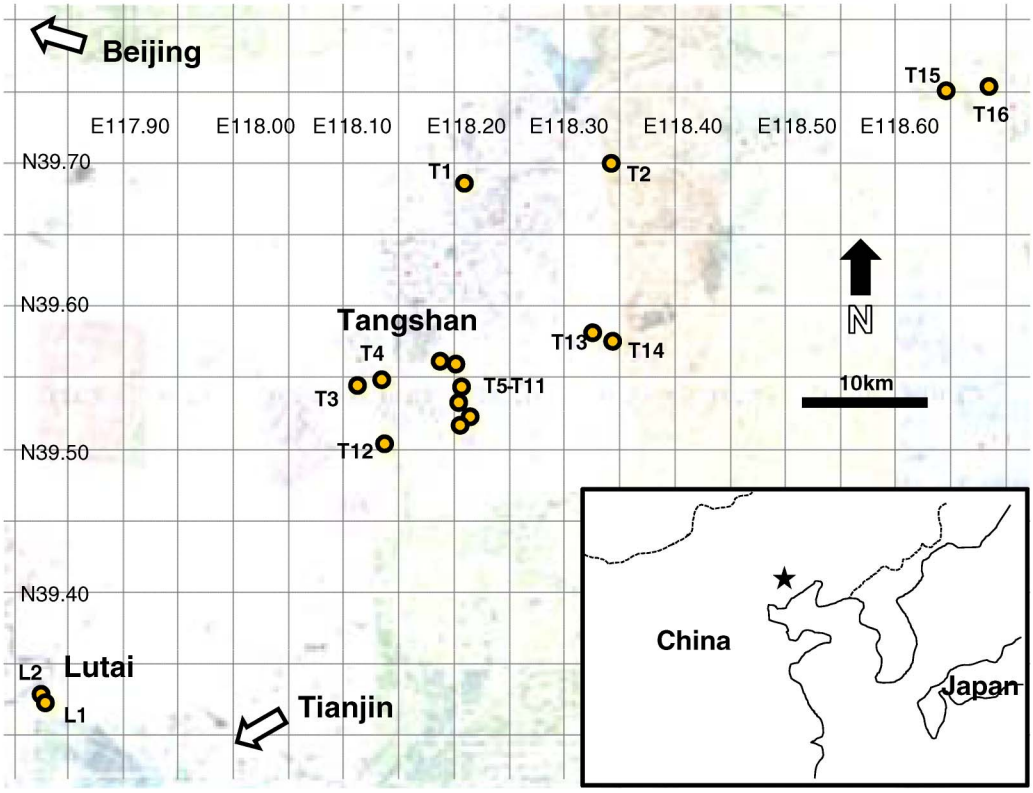

Fig. 4. Regional view of sites investigated; most of the sites are clustered around the city of Tangshan and are labeled with the letter T and the site number; sites located in the city of Lutai are labeled with the letter L and the site number

on the order of a few meters (e.g., this side of the pea patch or the other).

Confirmation of the right location was also assessed in a quantitative manner by observing the shape and trends in the 1978–1979 CPT soundings compared with to the 2007 soundings. Characteristic signatures of the site-specific stratigraphy were identified and used to confirm that the subsurface conditions between the two soundings were similar. A statistical analysis could have been used to provide a more quantitative analysis, but this was not deemed a worthwhile investment of time and labor for this project.

Fig. 4 shows a regional view of the site locations. Most of the sites are clustered in and around the city of Tangshan (labeled T), with two sites located to the southwest in Lutai (labeled L). The global positioning system (GPS) coordinates for each site are listed in Table 1 with WGS84 as the reference geoid. The letter and number site designation corresponds to the designation reported in Zhou and Zhang (1979) and Zhou and Guo (1979).

Case History Processing

The case histories from this investigation were processed according to the procedures outlined in Moss et al. (2006). These procedures account for the uncertainties in the load and resistance parameters by assessing their affect on the resulting liquefaction triggering correlation. Each processed case history was reviewed by at least three coauthors to ensure the quality and consistency of the analysis. These procedures result in a consistent and robust probabilistic estimate of cyclic loading and cyclic resistance for each site.

The depth to the water table is critical to liquefaction triggering analysis. For this study, the depth to the water table was based on the measurements made in 1978–1979. Water table uncertainty in Moss et al. (2006) was assumed to be a fixed or prescribed standard deviation of 0.3 m. For this study, because of the uncertainty of the original surface elevation to the current surface elevation and the uncertainty in the exact colocation of the previous and current borings, the fixed or prescribed standard deviation was increased to 0.5 m. The water table at many sites dropped several meters since the late 1970s because of regional groundwater pumping for agriculture, industrial, and residential use. Rebuilding after the 1976 earthquake stimulated the regional economy with an attendant growth in population and demand for water. Because the drop in the water table decreased the amount of near-surface saturated granular soil available for liquefaction, it is anticipated that liquefaction effects will be reduced throughout the region when the next large earthquake occurs.

The critical layer depth was based on the 1978–1979 measurements because they better represent the static stress conditions at the time of the earthquake. In some case histories, the surface elevation changed slightly since the previous measurements were recorded. This is probably a result of artificial processes, particularly agricultural practices, because most of the sites are agrarian in nature. For those cases, the critical layer trace was matched in the 2007 with the 1978–1979 soundings by using the characteristic shape of the trace. The 2007 CPT measurements were normalized by using the current stress conditions, and the resulting normalized resistance was used to represent the soil resistance at the time of the earthquake.

Over 30 years have transpired between the earthquake and these recent field investigations. Although this is a significant amount of time on a human scale, the geologic and engineering properties of the potentially liquefiable materials will have changed little. The water table dropped significantly, but this results in a change in the stress conditions, not necessarily a change in the soil's stress normalized penetration resistance. The changes in stress conditions were accounted for by using the 1978–1979 stress conditions for the cyclic stress ratio calculations and by using the 2007 stress conditions to normalize or remove the effects of overburden stress on the CPT measurements. Thirty years is too short of a duration to be concerned with the natural aging of the soil deposit with respect to liquefaction (Arango et al. 2000; Leon et al. 2005; Moss et al. 2008). The sites with high fines content may have experienced some amount of consolidation. However, for a site to be liquefiable, gravity forces and not colloidal forces control the physical response. And for gravity forces to control the response, the material must be made of some larger skeletal matrix of grains that would experience a very small amount of secondary compression since the Tangshan earthquake.

Comparing the 1978–1979 cone tip measurements with the 2007 cone tip measurements provided little insight into changes in the engineering properties of the soil or differences in the penetration resistance by using different cones. No observed systematic difference in the tip measurements existed. This is supported by Kulhawy and Mayne (1990) who found no systematic difference in tip measurements made by using different cones within the penetration resistance range (approximately 5–15 MPa) of most potentially liquefiable materials.

The magnitude of the event was measured by using surface waves with a reported magnitude of $M_s = 7.8$. By using the relationships presented in Heaton et al. (1986), converting the surface wave magnitude to a moment magnitude resulted in a magnitude $M_w = 7.89$. Uncertainty in the moment magnitude was established by using methods found in Moss et al. (2006).

Fig. 5 shows the 2007 log compared to the 1978–1979 log for site T1. The dotted line indicates the best estimate of the "critical layer" or the most potentially liquefiable layer in the soil profile. An English translation of the 1978–1979 log is provided. A slight difference in the elevation of the two logs exists; however, the characteristics of the subsurface profile as measured in the soundings agree nicely. The 1978–1979 cone measurements exhibited a blunted trace that is characteristic of these older cones that were less sensitive to variations in penetration resistance. The 1978–1979 log reported grain size but not the plastic and liquid limit (PI = LL-PL) of the fine-grained soil common in the United States. The effects of the fines content on the liquefiability of a soil deposit per Chinese code and the standard-of-practice in China is based solely on the clay fraction (0.005 mm) and not the plasticity and water content, which may result in an unconservative assessment of liquefaction in some cases (Moss and Chen 2008; Bray and Sancio 2006).

Tangshan Case Histories

Detailed reporting for each case history can be found in Moss et al. (2009), a Pacific Earthquake Engineering Research (PEER) data report. In that report, each case history has two or more pages documenting the pertinent calculations for determining the cyclic stress ratio (CSR) and cyclic resistance ratio (CRR). The results from the Tangshan district are presented here in Table 3 and from the Lutai District in Table 4.

The data processing techniques used for this analysis were the techniques developed by Moss et al. (2006) and explained in detail in the worldwide CPT database report by Moss et al. (2003). Table 3 lists, in order, the liquefied sites (Y), the sites that were removed because of some error in the data acquisition or other error (NA),

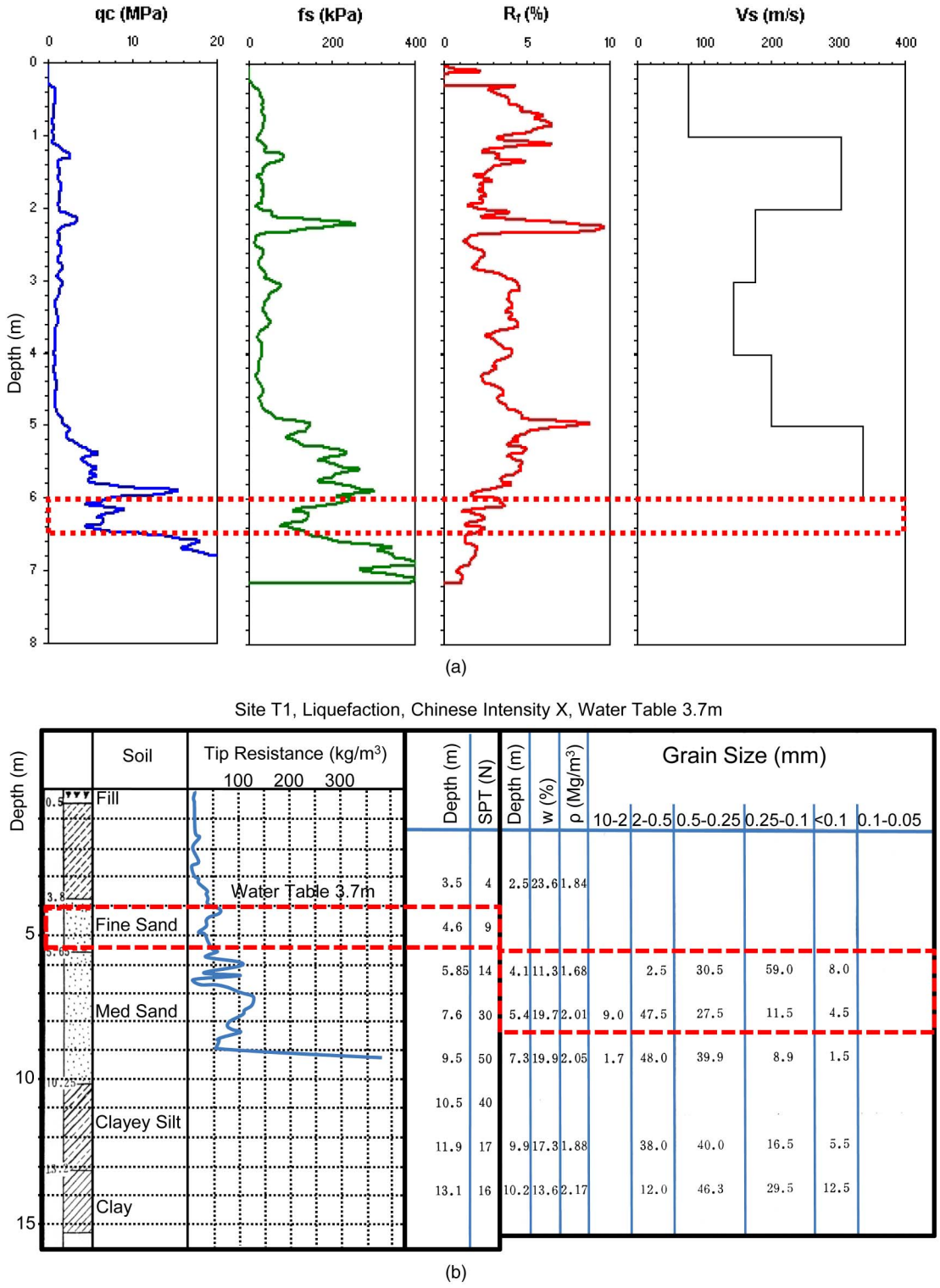

Fig. 5. (a) 2007 log performed by using a modern CPT measuring tip (qc), sleeve (fs), friction ratio (Rf), and shear wave velocity (VS); (b) 1978–1979 log performed by using SPT and now obsolete CPT; soil samples were collected for water content and grain size distribution analysis (data from Zhou and Zhang 1979)

and the nonliquefied sites (N). The 2007 subsurface conditions at Sites T3, T14, and T15 were not representative of the subsurface conditions as measured in 1978–1979 because the sites were not properly relocated, the sites were substantially modified in the interim, or other reasons; and therefore, these sites were removed from further consideration. Sites L1 and L2 were reassessed as cyclic failure of fine-grained soil and not liquefaction. A thorough discussion is presented subsequently.

Tangshan sites that were previously included in the Moss et al. (2003) database from Zhou and Zhang (1979) were those sites for which the critical layer was found to have less than a 5% fines content according to the soil samples obtained at the time.

Table 3. Median Case History Values for Tangshan District Sites

Site	Liquefied?	Data class	Median depth critical layer (m)	Median depth of groundwater table (m)	σ_{vo} (kPa)	σ'_{vo} (kPa)	a_{max} (g)	r_d	CSR	CSR*	q_{c1} (MPa)	R_f (%)	$q_{c1,mod}$ (MPa)
T1 Tangshan district	Y	C	4.75	3.70	83.38	73.07	0.64	0.82	0.39	0.42	6.85	2.27	8.79
T2 Tangshan district	Y	C	7.40	1.25	141.18	80.84	0.53	0.72	0.43	0.46	4.55	3.65	8.14
T6 Tangshan district	Y	C	5.10	1.50	95.70	60.38	0.64	0.8	0.53	0.57	12.37	0.86	12.81
T7 Tangshan district	Y	C	6.40	3.00	117.30	83.95	0.64	0.74	0.43	0.46	5.68	1.56	6.89
T8 Tangshan district	Y	C	5.25	2.20	96.88	66.95	0.64	0.79	0.48	0.51	10.37	0.84	10.77
T10 Tangshan district	Y	C	8.00	1.45	152.38	88.12	0.64	0.66	0.47	0.51	5.86	1.88	7.48
T11 Tangshan district	Y	C	2.10	0.85	38.83	26.56	0.61	0.94	0.54	0.58	6.65	1.36	7.71
T12 Tangshan district	Y	C	3.10	1.55	56.58	41.37	0.58	0.90	0.47	0.50	3.20	1.33	4.17
T13 Tangshan district	Y	C	7.00	1.05	133.88	75.51	0.58	0.72	0.48	0.52	14.12	0.96	14.67
T14 Tangshan district	NA	C	1.80	1.25	31.98	26.58	0.54	0.95	0.40	0.43	17.30	0.77	17.59
T15 Tangshan district	NA	C	2.40	1.00	44.3	30.57	0.27	0.95	0.24	0.26	16.18	0.74	16.40
T3 Tangshan district	NA	C	6.80	1.50	97.16	61.11	0.64	0.72	0.47	0.51	7.17	3.05	10.16
T4 Tangshan district	N	C	3.40	1.10	63.55	40.99	0.64	0.87	0.56	0.61	16.26	1.07	16.96
T5 Tangshan district	N	C	4.50	3.00	80.25	65.54	0.64	0.83	0.42	0.46	12.58	1.06	13.22
T9 Tangshan district	N	C	4.00	1.10	75.25	46.80	0.64	0.86	0.57	0.62	17.16	0.83	17.58
T16 Tangshan district	N	C	7.50	3.50	137.50	98.26	0.26	0.78	0.19	0.20	10.88	0.94	11.24

Table 4. Median Case History Values for Lutai District Sites

Site	Liquefied?	Data class	Median depth critical layer (m)	Median depth of groundwater table (m)	σ_{vo} (kPa)	σ'_{vo} (kPa)	a_{max} (g)	r_d	CSR	CSR*	q_{c1} (MPa)	R_1 (%)	$q_{c1,mod}$ (MPa)	CSR^*_{cyclic}	CRR_{cyclic}
L1 Lutai district	N?	C	9.75	0.40	189.13	97.40	0.27	0.70	0.24	0.25	3.60	1.71	4.70	0.26	0.24
L2 Lutai district	Y?	ERR	12.50	0.21	243.23	122.66	0.27	0.63	0.22	0.24	3.32	1.31	4.03	0.26	0.17

Note: The failure mechanism is conjectured to be cyclic failure and not liquefaction for these cases; therefore, they should not be included in the liquefaction database.

Sleeve measurements were then not necessary to account for the influence of the fines on the liquefaction resistance, and the sites with the sleeveless cone measurements could be used. The data for Sites T1, T2, T8, and T10 that were included in Moss et al. (2003) have been reinvestigated and revised as a result of the recent field work. Sites T3, T4, T5, T6, T7, T9, T11, T12, T13, T14, T15, and T16 were not included in Moss et al. (2003) and have now been added to the database. Listed in Table 2 are Sites F13, T19, T21, T22, T30, T32, T36, Y21, Y24, Y28, and Y29 from Moss et al. (2003) that were not reinvestigated in this field work and are considered still valid case histories with the revision of the PGA estimates as recommended for consistency with the other case histories from this earthquake.

The common headers in Tables 3 and 4 are

- Site designated by letter and number per district;
- Occurrence of liquefaction (Y/NA/N);
- Data class set by Moss et al. (2006) criteria;
- Median depth of critical layer estimated for the time of the earthquake;
- Median depth of groundwater table (GWT) estimated for the time of the earthquake;
- σ_{vo} the total vertical stress;
- σ_{vo} the effective vertical stress;
- a_{max} the peak ground acceleration;
- r_d the nonlinear shear mass participation factor;
- CSR the simplified cyclic stress ratio;
- CSR* the simplified cyclic stress ratio corrected to a moment magnitude of 7.5;
- q_{c1} the median overburden corrected tip resistance over the critical layer;
- R_f the median friction ratio over the critical layer; and
- $q_{c1,mod}$ the "apparent" fines corrected median tip resistance.

In Table 4, CSR^*_{cyclic} and CRR_{cyclic} are the terms used by Boulanger and Idriss (2006) to define the cyclic stress ratio and cyclic resistance ratio of claylike soils susceptible to cyclic failure. The coefficient of variation of CSR for Site L2 exceeds the acceptable criteria for uncertainty; and therefore, the data class column contains "ERR," and this site was removed from the liquefaction database.

The summary of case history results are plotted against the probabilistic liquefaction triggering curves presented in Moss et al. (2006). Figs. 6–8 show the processed liquefaction and nonliquefaction case histories against the probabilistic triggering curves and the existing worldwide database. The Tangshan district case histories are shown as squares and the Lutai district case histories are shown as triangles. The Tangshan sites agree well with the existing probabilistic triggering curves. The most valuable result from this study, and what drove the research effort, was acquiring the three nonliquefied sites in the high CSR range. This data region is poorly

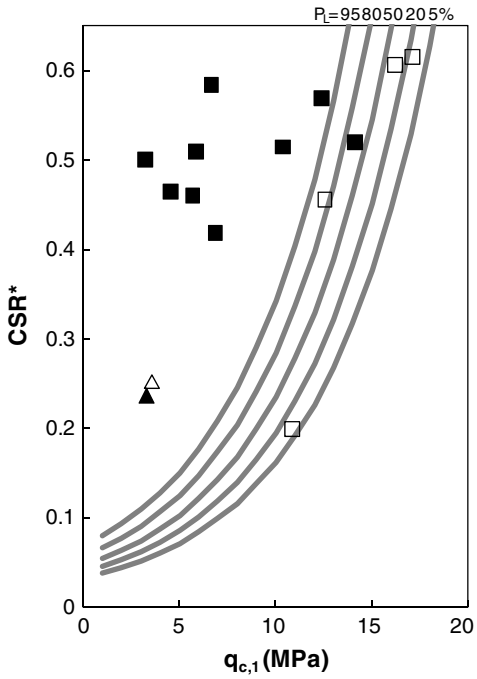

Fig. 6. Tangshan district (squares) and Lutai district (triangles) case histories shown against the Moss et al. (2006) probabilistic liquefaction triggering curves; *x*-axis is the cone-tip resistance normalized for effective overburden pressure; *y*-axis is the cyclic stress ratio corrected for magnitude

populated and any high CSR nonliquefied site is extremely valuable for constraining the upper portion of the triggering curves.

Sites L1 and L2 lie well to the left of the triggering curves and the liquefaction and nonliquefaction cases have similar overburden corrected and apparent fines-corrected tip resistance. This characteristic curve offset has been observed in similar cases for which ground deformations (similar to postliquefaction effects) were recorded, but the soil failed in cyclic failure as discussed by Boulanger and Idriss (2006). This was the situation for some 1999 Chi Chi, Taiwan Wufeng sites (Chu et al. 2008) and for some 1999 Kocaeli, Turkey Adapazari sites (Bray et al. 2004) as analyzed for the Moss et al. (2003) CPT database. For the two Lutai sites, the cyclic resistance ratio CRR_{cyclic} of claylike soil based on penetration resistance-derived s_u (undrained strength) was calculated by using Boulanger and Idriss (2006). In comparing the CRR/CSR* liquefaction ratio to the $CRR_{cyclic}/CSR^*_{cyclic}$ cyclic failure ratio, cyclic failure has a much lower factor of safety than liquefaction, indicating that cyclic failure is the more likely failure mechanism.

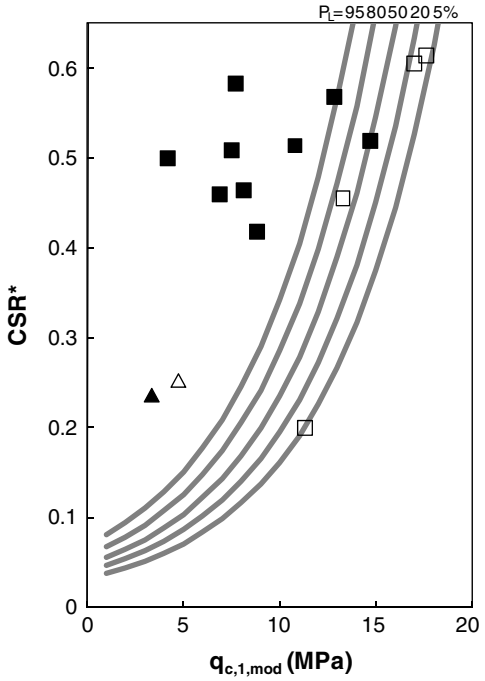

Fig. 7. Similar to Fig. 6 with the exception that *x*-axis shows the cone-tip resistance that has been modified for "apparent" fines content by using the friction ratio for a proxy

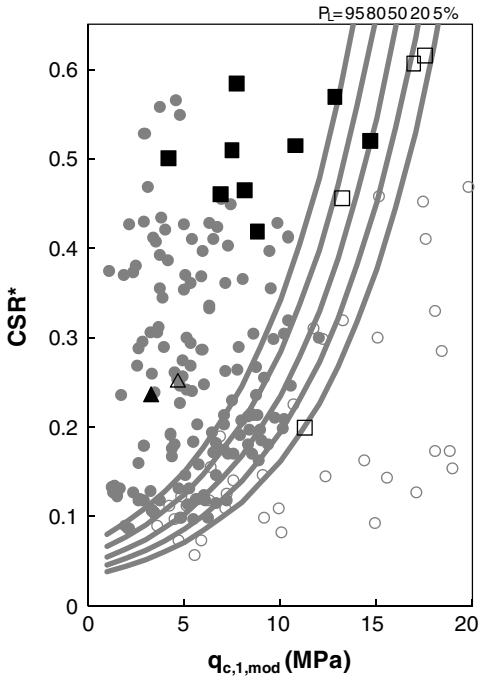

Fig. 8. Tangshan district and Lutai district case histories in relationship to the worldwide CPT case history database (Moss et al. 2003); the Tangshan district sites are particularly important because of the high CSR values and nonliquefaction cases; the Lutai district sites are interpreted to be an example of cyclic failure and not liquefaction

Zhou and Guo (1979) observed clay boils at L2, which is possible given the increase in excess pore pressures and reduced soil strength associated with cyclic failure. Cyclic failure is highly dependent on static driving shear stresses, which is commonly called the K_α effect (Youd et al. 2001). It is conjectured that L2 experienced higher static driving shear stresses than L1 because of larger building loads that led to the manifestation of ground deformations and/or soil ejecta. This is the case at the sites today with larger building loads at L2; however, this is only conjecture for the time of the earthquake because no information about the relative size and loading of the structures circa 1976 exists. The determination that the failure mechanism was cyclic failure is supported by the Atterberg limits of a sample obtained from L1, which indicated a plasticity index (PI) of 36. A grain size analysis for the same sample showed that approximately 87% of the material was smaller than 0.075 mm (fines content), and approximately 32% of the material was smaller than 0.005 mm (clay fraction). These grain size and colloidal force measurements place the sample material well outside the range of measurements for material that would fail in a manner consistent with the physics of liquefaction and solidly in the cyclic failure realm.

Summary

A reinvestigation of selected liquefaction and nonliquefaction sites from the 1976 Tangshan earthquake was recently performed. The goal of this collaborative effort was to collect CPT data at sites where an obsolete cone was used for subsurface investigations following the earthquake. In total, 18 sites were successfully reinvestigated, and of these, 13 were considered accurate representative case histories. A pair of case histories that were originally investigated as liquefaction have been reassessed as cyclic failure of fine grained soil and have been removed from consideration in the liquefaction database. The most valuable results from this study were the three nonliquefaction case histories with high CSR that help fill the poorly populated region of the liquefaction triggering database. These three nonliquefaction case histories warrant the significant effort expended to acquire this information and will be useful in the future assessment of probabilistic liquefaction triggering curves.

This study adds to the ever-increasing database for evaluating the threshold between liquefaction and nonliquefaction. The difficulty and cost associated with documenting the liquefaction phenomena makes every case history valuable. The field of liquefaction engineering is maturing and today, general agreement among different studies as to the median location of liquefaction triggering curves exists. The new and revised data presented in this study probably will have only a slight (most likely negligible) affect on the median location of future triggering curves. However, this data will affect the uncertainty bounds of triggering curves and will better constrain the upper range of the liquefaction triggering threshold. This will be useful as earthquake engineers embrace the probabilistic approach of performance-based design and grapple with future events that push the limits of our analysis methods.

Acknowledgments

This research was a collaborative effort between researchers in the United States and researchers in China. The research was directed by Robb Moss (Cal Poly San Luis Obispo) with assistance from Robert Kayen (USGS). Southeast University in Nanjing, China, provided the ground support with a fully staffed CPT rig, lab support for analyzing soil samples, and analytical support in the data reduction. Collaborators from Southeast University included Professor Liu, Professor Tong, Professor Du, and Guojun Cai. The China Earthquake Agency (CEA) in conjunction with Institute Engineering Mechanics (IEM) in Harbin provided logistical support and assistance in locating and obtaining access to the sites.

Collaborators from CEA-IEM included Professor Yuan, Professor Tow, Cao Zhengzhong, Dr. Shi Lijing, and several student researchers. This research was truly a collaborative effort and would not have been successful without the contribution from every member of the team.

This work was supported by the National Science Foundation under SGER Grant No. 0633886. Funding in China was provided by the National Natural Science Foundation of China (NSFC) Grant No. 40702047 and the Jiangsu Transportation Research Foundation Grant No. 8821006021. The writers are thankful for the funding and the opportunity to pursue this research. Any opinions, findings, and conclusions or recommendations expressed are those of the writers and do not necessarily reflect the views of the funding agencies.

References

Arango, I., Lewis, M. R., and Kramer, C. (2000). "Updated liquefaction potential analysis eliminates foundation retrofitting of two critical structures." *Soil Dyn. Earthquake Eng.*, 20(1–4), 17–25.

Atkinson, G. M., and Boore, D. M. (1995). "New ground motion relations for eastern North America." *Bull. Seismol. Soc. Am.*, 85(1), 17–30.

Atkinson, G. M., and Boore, D. M. (1997). "Some comparisons between recent ground motion relations." *Seismol. Res. Lett.*, 68(1), 24–40.

Boulanger, R. W., and Idriss, I. M. (2006). "Liquefaction susceptibility criteria for silts and clays." *J. Geotech. Geoenviron. Eng.*, 132(11), 1413–1426.

Bray, J. D., et al. (2004). "Subsurface characterization at ground failure sites in Adapazari, Turkey." *J. Geotech. Geoenviron. Eng.*, 130(7), 673–685.

Bray, J. D., and Sancio, R. B. (2006). "Assessment of the liquefaction susceptibility of fine-grained soils." *J. Geotech. Geoenviron. Eng.*, 132(9), 1165–1177.

Chu, D. B., Stewart, J. P., Boulanger, R. W., and Lin, P. S. (2008). "Cyclic softening of low-plasticity clay and its effect on seismic foundation performance." *J. Geotech. Geoenviron. Eng.*, 134(11), 1595–1608.

Dahle, A., Bungum, H., and Dvamme, L. G. (1990). "Attenuation models inferred from intraplate earthquake recordings." *Earthquake Eng. Struct. Dyn.*, 19(8), 1125–1141.

Heaton, T. C., Tajima, F., and Mori, A. W. (1986). "Estimating ground motions using recorded accelerograms." *Surv. Geophys.*, 8(1), 25–83.

Kayen, R. E., Tao, X., Shi, L , and Shi, H. (2008). "Shear wave velocity investigation of soil liquefaction sites from the Tangshan, China M7.8 earthquake of 1976 using active and passive surface wave methods." *Proc., 6th Int. Conf. on Case Histories in Geotechnical Engineering*, Missouri Univ. of Science and Technology, Rolla, MO.

Kulhawy, F. H., and Mayne, P. W. (1990). "Manual on estimating soil properties for foundation design." *Rep. EL-6800*, Electric Power Research Institute, Palo Alto, CA.

Leon, E., Gassman, S. L., and Talwani, P. (2005). "Effect of soil aging on assessing magnitude and accelerations." *Earthquake Spectra*, 21(3), 737–759.

Liu, H., Housner, G. W., Xie, L., and He, D. (2002). "The great Tangshan earthquake of 1976." *Technical Rep.: CaltechEERL:EERL.2002.001*, Earthquake Engineering Research Library, California Institute of Technology, Pasadena, CA, ⟨http://caltecheerl.library.caltech.edu/353/⟩ (Jul. 10, 2008).

Moss, R. E. S., and Chen, G. (2008). "Comparing liquefaction procedures in the U.S. and China." *Proc., 14th World Conf. on Earthquake Engineering*, International Association for Earthquake Engineering (IAEE), Beijing.

Moss, R. E. S., Collins, B. D., and Whang, D. H. (2005). "Retesting of liquefaction/nonliquefaction case histories in the imperial valley." *Earthquake Spectra*, 21(1), 179–196.

Moss, R. E. S., Kayen, R. E., Tong, L.-Y., Liu, S.-Y., Cai, G.-J., and Wu, J. (2009). "Re-investigation of liquefaction and nonliquefaction case histories from the 1976 Tangshan earthquake." *Rep. No. 209/102*, Pacific Earthquake Engineering Research (PEER) Center, Berkeley, CA.

Moss, R. E. S., Seed, R. B., Kayen, R. E., Stewart, J. P., Der Kiureghian, A., and Cetin, K. O. (2006). "Probabilistic seismic soil liquefaction triggering using the CPT." *J. Geotech. Geoenviron. Eng.*, 132(8), 1032–1051.

Moss, R. E. S., Seed, R. B., Kayen, R. E., Stewart, J. P., Youd, T. L., and Tokimatsu, K. (2003). "Field case histories for CPT-based in situ liquefaction potential evaluation." *Berkeley Geoengineering Research Rep. No. UCB/GE-2003/04*, Univ. of California, Berkeley, CA.

Moss, R. E. S., Thornhill, D. M., Nelson, A. I., and Levulett, D. A. (2008). "Influence of aging on liquefaction potential: Preliminary results." *Proc., ASCE Conf. Geotechnical Earthquake Engineering and Soil Dynamics IV*, Reston, VA.

Seed, H. B., Tokimatsu, K., Harder, L. F., and Chung, R. M. (1985). "Influence of SPT procedures in soil liquefaction resistance evaluations." *J. Geotech. Eng.*, 111(12), 1425–1445.

Shengcong, F., and Tatsuoka, F. (1984). "Soil liquefaction during Haicheng and Tangshan earthquake in China: A review." *Soils Found.*, 24(4), 11–29.

Shibata, T., and Teparaska, W. (1988). "Evaluation of liquefaction potential of soils using cone penetration testing." *Soils Found.*, 28(2), 49–60.

Stewart, J. P., Liu, A. H., and Choi, Y. (2003). "Amplification factors for spectral acceleration in tectonically active regions." *Bull. Seismol. Soc. Am.*, 93(1), 332–352.

Toro, G. R., Abrahamson, N. A., and Schneider, J. F. (1997). "Model of strong ground motions from earthquakes in central and eastern North America: Best estimates and uncertainties." *Seismol. Res. Lett.*, 68(1), 41–57.

Youd, T. L., et al. (2001). "Liquefaction resistance of soils: Summary report from the 1996 NCEER and 1998 NCEER/NSF workshops on evaluation of liquefaction resistance of soils." *J. Geotech. Geoenviron. Eng.*, 127(10), 817–833.

Zhou, S. G., and Guo, L. J. (1979). "Liquefaction investigation in Lutai district." Ministry of Railway, Beijing (in Chinese).

Zhou, S. G., and Zhang, S. M. (1979). "Liquefaction investigations in Tangshan district." Ministry of Railway, Beijing (in Chinese).